

## Using High Resolution Global Atmospheric Simulations to Investigate Gravity Wave Impact on Infrasound Transmission Losses Across the International Monitoring System

C. Listowski<sup>1</sup>, C. Stephan<sup>2</sup>, A. Le Pichon<sup>1</sup>, A. Hauchecorne<sup>3</sup>, Y.-H. Kim<sup>4</sup>,  
U. Achatz<sup>4</sup>, and G. Bölöni<sup>5</sup>

<sup>1</sup>CEA/DAM, France <sup>2</sup>MPIM, Germany <sup>3</sup>LATMOS, France <sup>4</sup>GUF, Germany <sup>5</sup>DWD, Germany



### INTRODUCTION

Gravity waves (GW) alter the propagation path of infrasound waves in the middle atmospheric waveguide.

Working with models explicitly resolving GW, we aim at quantifying the impact of GW on surface transmission losses (TLoss) across the IMS.

### METHODS/DATA

Data/Tools we use:

- High resolution atmospheric simulation outputs (Jan-Feb 2020)
- Rayleigh lidar data
- Satellite observations of GW potential energy
- Propagation simulations using atmospheric specifications where GW are kept in / filtered out

START

### RESULTS

Stratospheric GW extracted from simulations are consistent with observed GW perturbations at the lidar station and across IMS as inferred from satellite.

Propagation simulations show an average of up to 40 (10) dB TLoss difference at IMS stations at 1 (0.1) Hz.

### CONCLUSION

A method is proposed to quantify stratospheric GW impact at the IS stations.

Validation of the modelled GW perturbations against obs. is achieved.

There is much larger impact of GW at 1 Hz than at 0.1 Hz.

There is no systematic link between GW impact on TLoss and GW energy (latitude) across the IMS.

Please do not use this space, a QR code will be automatically overlaid



- IMS detection capability with infrasound technology builds upon relevant estimations of transmission losses at the surface across the network throughout the year (Figure 1).

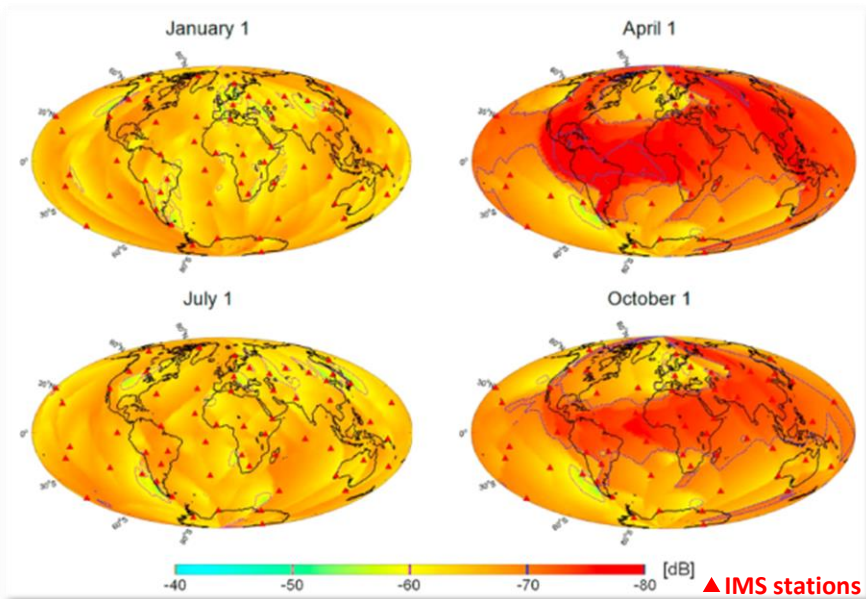


Figure 1. Smallest signal attenuation expected at 0.8Hz with a 2-station coverage (Le Pichon et al. 2012) using IFS/ECMWF (-60 dB is a factor of 1000 in amplitude.)

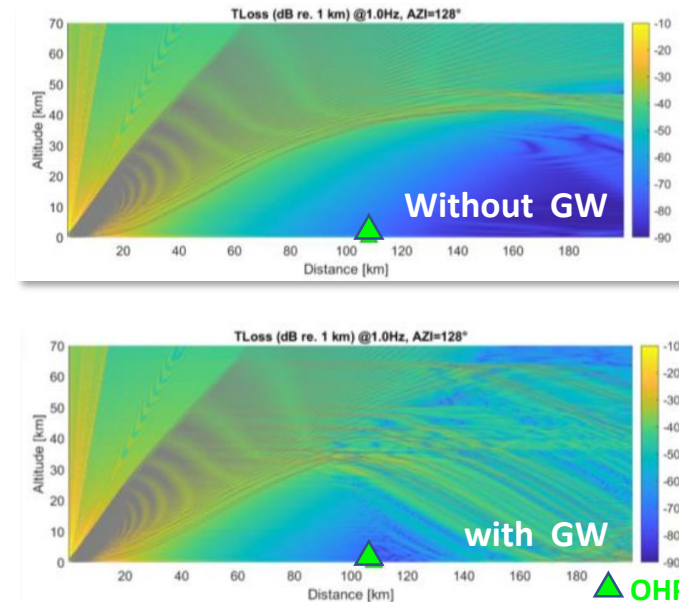


Figure 2. Explaining infrasound detection of Le Teil's earthquake at Observatoire de Haute Provence (OHP) (Vallage et al. 2021)

- Gravity waves (GW) significantly alter the propagation path of infrasound waves in the middle atmospheric waveguide through partial reflections in the shadow zones (Figure 2), or through the temporary setting of a new stratospheric geometric waveguide.
- However GW are often poorly resolved in atmospheric specifications despite their estimated significant effect on detection thresholds (up to factor of 5-10 on the amplitude) *Le Pichon et al. 2019*

- In the literature, there are different ways of investigating/accounting for the impact of GW in infrasound propagation simulations:
  - Parameterizations based on the GW universal spectrum *e.g. Gardner et al. 1993, as in Vallage et al. 2021*
  - Stochastic parameterizations accounting for GW intermittency *e.g. de la Camara et al., 2015 as in Cugnet et al. 2019*
  - GW ray-tracing equations applied to a frequency spectrum *e.g. Drob et al. 2013*
  - 3D GW-spectrum model *Chunchuzov & Kulichkov, 2019*
- Working with high-resolution  $O(1 \text{ km})$  models explicitly resolving a large part of the GW spectrum - without using GW parameterizations - is another way, given increased computing means.
- We use a dataset of a high-resolution model runs' outputs to demonstrate a method for quantifying the systematic impact of GW across IMS stations, based on transmission losses (TLoss) calculations.



INTRODUCTION

OBJECTIVES

METHODS/DATA

RESULTS

CONCLUSION



Please do not use this space, a QR code will be automatically overlaid

P1.1-675



## Data

### DYAMOND dataset *Stevens et al. 2019, phase II* *Stephan et al. 2022*

Model : ICON *Zängl et al. 2015*

Period: 20 Jan. – 29 Feb. 2020 (3-hourly outputs)

Initialization : ECMWF/IFS ; freely-running

Model top : 75km (45 km: avoiding sponge layer)

Configurations:

- dpp0029: dx = 5km (regridded: 0.35° x 0.35°)
- nwp2.5winter: dx = 2.5km (regridded: 0.35° x 0.35°)

### Rayleigh lidar observations at OHP *e.g. Hauchecorne et al. 1980*

Observatoire de Haute Provence, France (LATMOS)

**Altitude range:** 30-90km ; **Vertical resolution :** 75 m ;

**Accuracy:** < 1K (below 70km altitude)

**Data:** 16 night profiles (4 hourly-average)

### Satellite observations: GRACILE dataset *Ern et al. 2018*

IR limb sounders HIRDLS (2005-2008) and SABER (2002-2015)

→ zonal averages of Ep (mean, max, min),  $\text{Dlat}_{\text{hirdls/saber}} = 2.5^\circ/5^\circ$

## Method

### GW extraction for field $X=U,V,T$

- ICON outputs interpolated on a vertical grid with  $dz=1.5\text{km}$  to match average  $dz$  in the stratosphere
- background  $X_{\text{back}}$  obtained by filtering out  $\lambda_z < 15\text{ km}$  (3<sup>rd</sup> order Butt. filt.) in T  
*e.g. Baumgarten et al., 2017*
- deriving GW perturbation:  $X - X_{\text{back}} = \Delta T$

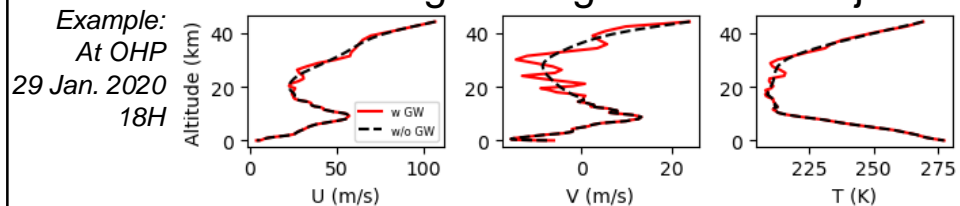
### Atmospheric specifications for IS

Altitude: sticking to 0-45 km only

→ avoiding artefacts from upper interpolation with other model

Filtering: only applied in the stratosphere

→ avoiding filtering out low level jets



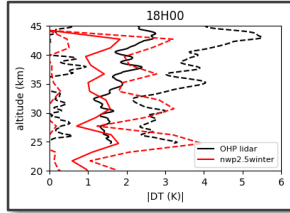
## Infrasound propagation simulations

Range-independant PE simulations done with NCPAprop *Waxler & Assink, 2019* at OHP and IMS stations

**Deriving TLoss differences** between PE simulation using specifications w and w/o GW, respectively

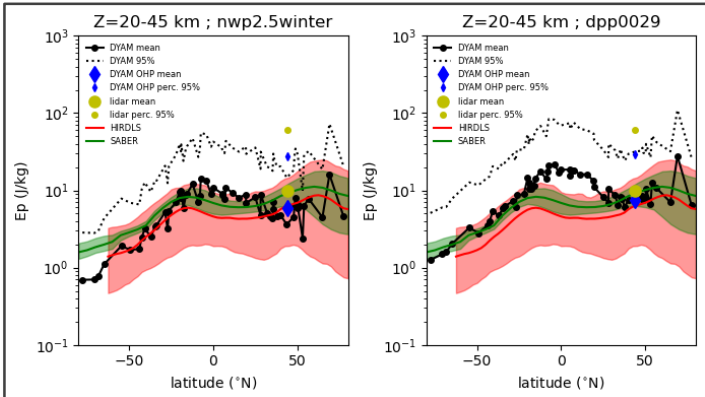
# Results: stratospheric GW across the IMS and impact on transmission loss

GW perturbations derived from model are consistent with lidar and satellite observations ( $E_p$ ).



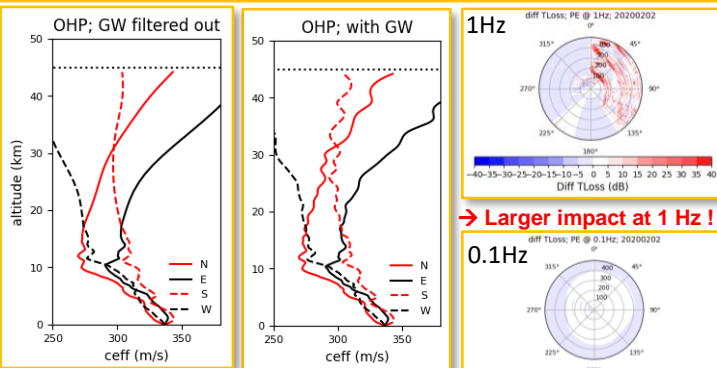
GW potential energy

$$E_p = \frac{1}{2} \left( \frac{g}{N} \right)^2 \left( \frac{\Delta T}{T} \right)^2$$

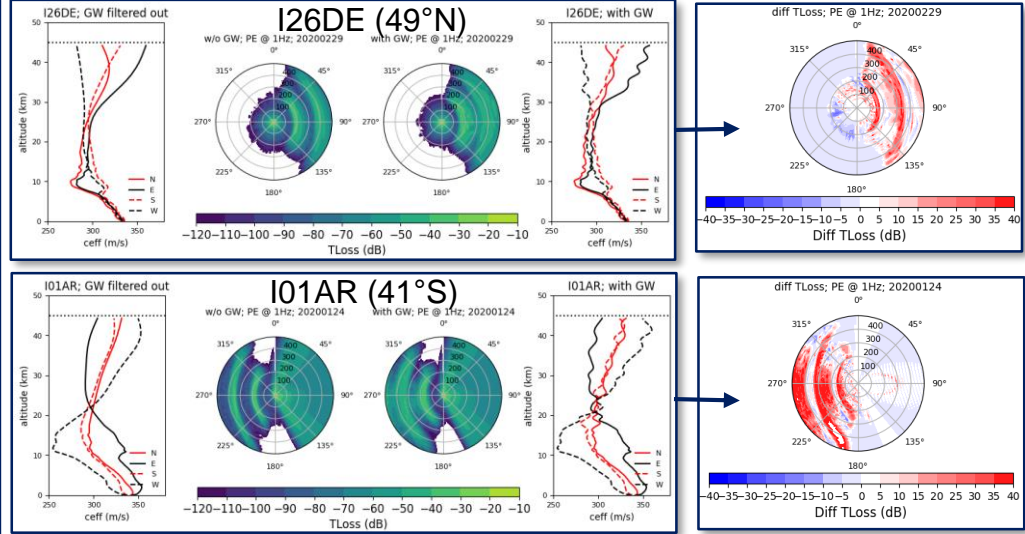


→ nwp2.5winter is then used for simulating TLoss

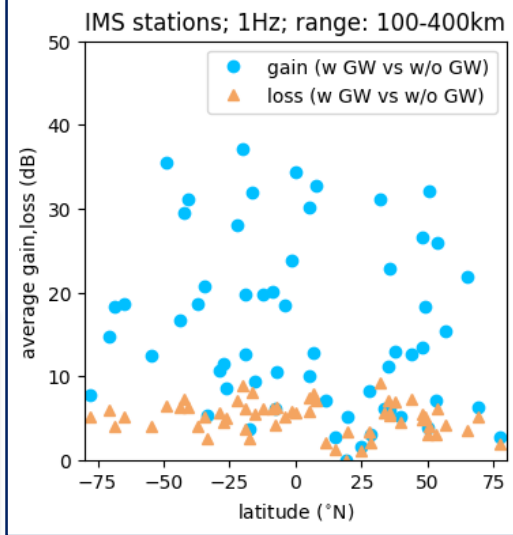
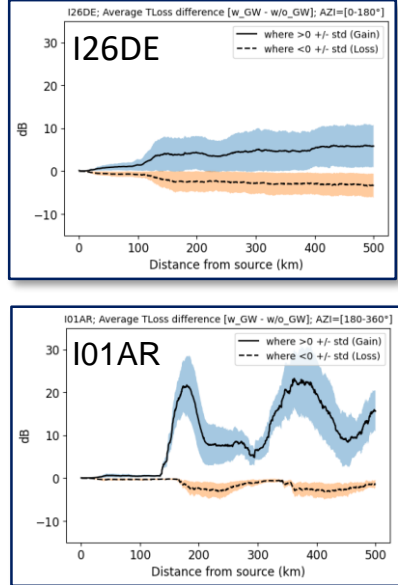
**Definition:** Diff TLoss = TLoss<sub>w/GW</sub> - TLoss<sub>w/o GW</sub>



**GW impact on the stratospheric guide:**  
 e.g filling the shadow zone, setting new geometric guides, enlarging guides (larger azi.range)



**GW impact vs. distance** depends on the station (hemisphere,...) .  
 Gain = diff TLoss >0  
 Loss = diff TLoss <0  
 (difference considered only where TLoss<sub>w/GW</sub> is > -60 dB)  
**GW impact vs. latitude** or vs. GW energy (wrt top left figure): no pattern.



Gain at 1 Hz ~ 10-40 dB

- INTRODUCTION
- OBJECTIVES
- METHODS/DATA
- RESULTS
- CONCLUSION



Please do not use this space, a QR code will be automatically overlaid



- We demonstrate a method for **quantifying the systematic impact of stratospheric GW across IMS stations**, based on TLoss calculations with **PE simulations**.
- We use a database of state of the art high-resolution model outputs where **GW are not parameterized**.
- We **validate the modelled GW perturbations using Rayleigh lidar data** at Observatoire de Haute-Provence.
- We **validate the modelled GW amplitudes using satellite products across the IMS** based on the GW potential energy ( $E_p$ ).
- The **average impact of GW is much larger at 1 Hz** (TLoss increase of **up to 40 dB**) than at 0.1 Hz (less than 10 dB).
- **The impact of GW versus distance-to-station** depends on the considered IMS station (hemisphere) with a more or less pronounced impact on the shadow zone. There is **no systematic link between GW impact on TLoss and GW energy** (latitude). This points at the complex intrication of small-scale structure's role with that of the larger-scale variability (main stratospheric guide).



INTRODUCTION

OBJECTIVES

METHODS/DATA

RESULTS

CONCLUSION



Please do not use this space, a QR code will be automatically overlaid

P1.1-675

- Baumgarten, K., Gerding, M., & Lübken, F. J. (2017). Seasonal variation of gravity wave parameters using different filter methods with daylight lidar measurements at midlatitudes. *Journal of Geophysical Research: Atmospheres*, 122(5), 2683-2695.
- de la Camara, F. Lott, « A parameterization of gravity waves emitted by fronts and jets », *Geophys. Res. Lett.*, 42, p. 2071-2078 (2015).
- Chunchuzov, I., & Kulichkov, S. (2019). Internal gravity wave perturbations and their impacts on infrasound propagation in the atmosphere. In *Infrasound Monitoring for Atmospheric Studies* (pp. 551-590). Springer, Cham.
- Cugnet, A. De La Camara, F. Lott, C. Millet, B. Ribstein, (2018), « Non-orographic gravity waves : representation in climate models and effects on infrasound », dans A. Le Pichon, É. Blanc,
- Drob, D. P., D. Broutman, M. A. Hedlin, N. W. Winslow, and R. G. Gibson (2013), A method for specifying atmospheric gravity wavefields for long-range infrasound propagation calculations, *J. Geophys. Res. Atmos.*, 118, 3933–3943,
- Gardner, C. S., C. A. Hostetler, and S. J. Franke (1993), Gravity wave models for the horizontal wave number spectra of atmospheric velocity and density fluctuations, *J. Geophys. Res.*, 98, 1035-1049
- Hauchecorne, A., and M. L. Chanin (1980), Density and temperature profiles obtained by lidar between 35 and 70 km, *Geophys. Res. Lett.*, 7(8), 565–568, doi:10.1029/GL007i008p00565.
- Ern, M., Trinh, Q. T., Preusse, P., Gille, J. C., Mlynczak, M. G., Russell III, J. M., and Riese, M.: GRACILE: a comprehensive climatology of atmospheric gravity wave parameters based on satellite limb soundings, *Earth Syst. Sci. Data*, 10, 857–892, <https://doi.org/10.5194/essd-10-857-2018>, 2018.
- Le Pichon, A., L. Ceranna, and J. Vergoz (2012), Incorporating numerical modeling into estimates of the detection capability of the IMS infrasound network, *J. Geophys. Res.*, 117, D05121, doi:10.1029/2011JD016670.
- Le Pichon, A., Ceranna, L., Vergoz, J., & Tailpied, D. (2019). Modeling the detection capability of the global IMS infrasound network. In *Infrasound Monitoring for Atmospheric Studies* (pp. 593-604). Springer, Cham
- Stephan, CC, Duras, J, Harris, L,Klocke, D, Putman, WM, Taylor, M, Wedi, NP, Žagar, N and Ziemer, F. 2022. Atmospheric Energy Spectra in Global Kilometre-Scale Models. *Tellus A: Dynamic Meteorology and Oceanography*, 74(2022): 280–299. DOI: <https://doi.org/10.16993/tellusa.26>
- Stevens, B., Satoh, M., Auger, L., Biercamp, J., Bretherton, C. S., Chen, X., ... & Kodama, C. (2019). DYAMOND: The DYnamics of the atmospheric general circulation modeled on non-hydrostatic domains. *Progress in Earth and Planetary Science*, 6(1), 61.
- Waxler, R., & Assink, J. (2019). Propagation modeling through realistic atmosphere and benchmarking. *Infrasound monitoring for atmospheric studies: Challenges in middle atmosphere dynamics and societal benefits*, 509-549.
- Vallage et al. (2021) Multitechnology characterization of an unusual surface rupturing intraplate earthquake: the ML 5.4 2019 Le Teil event in France, *Geophysical Journal International*, Volume 226, Issue 2, August 2021, Pages 803–813
- Zängl, G., D. Reinert, P. Ripodas, and M. Baldauf (2015): The ICON (icosahedral non-hydrostatic) modelling framework of DWD and MPI-M: Description of the non-hydrostatic dynamical core. *Quart. J. Roy. Meteor. Soc.*, 141, 563–579



INTRODUCTION

OBJECTIVES

METHODS/DATA

RESULTS

CONCLUSION



Please do not use this space, a QR code will be automatically overlaid

P1.1-675